

TEMPLATE STRATEGY FOR THE SYNTHESIS OF Cu_2O -Pt HIERARCHICAL HETEROSTRUCTURES FOR THE DEGRADATION OF METHYLENE BLUE

SHIYONG BAO, HAN ZHU, PAN WANG and MEILING ZOU
*Faculty of Materials and Textiles, Zhejiang Sci-Tech University
Hangzhou 310018, P. R. China*

MINGLIANG DU* and MING ZHANG
*Faculty of Materials and Textiles, Zhejiang Sci-Tech University
Hangzhou 310018, P. R. China*

*Key Laboratory of Advanced Textile Materials
and Manufacturing Technology, Zhejiang Sci-Tech University
Ministry of Education, Hangzhou 310018, P. R. China
du@zstu.edu.cn

Received 2 May 2013

Accepted 28 June 2013

Published 18 September 2013

A facile and green route was introduced to synthesize Pt nanoparticles (PtNPs) immobilized on Cu_2O octahedrons to form Cu_2O -Pt hierarchical heterostructure. Transmission electron microscopy (TEM), field emission scanning electron microscopy (FE-SEM), high resolution transmission electron microscopy (HRTEM), X-ray photoelectron spectroscopy (XPS) and X-ray diffraction (XRD) were employed to study their morphology, chemical and crystallographic properties of the Cu_2O -Pt hierarchical heterostructure. These novel Cu_2O -Pt hierarchical heterostructures show fascinating degradations of methylene blue (MB), due to the suppressed electron/hole recombination phenomena and the efficient ability to capture the light.

Keywords: Cu_2O octahedron; Cu_2O -Pt hierarchical heterostructure; degradation.

1. Introduction

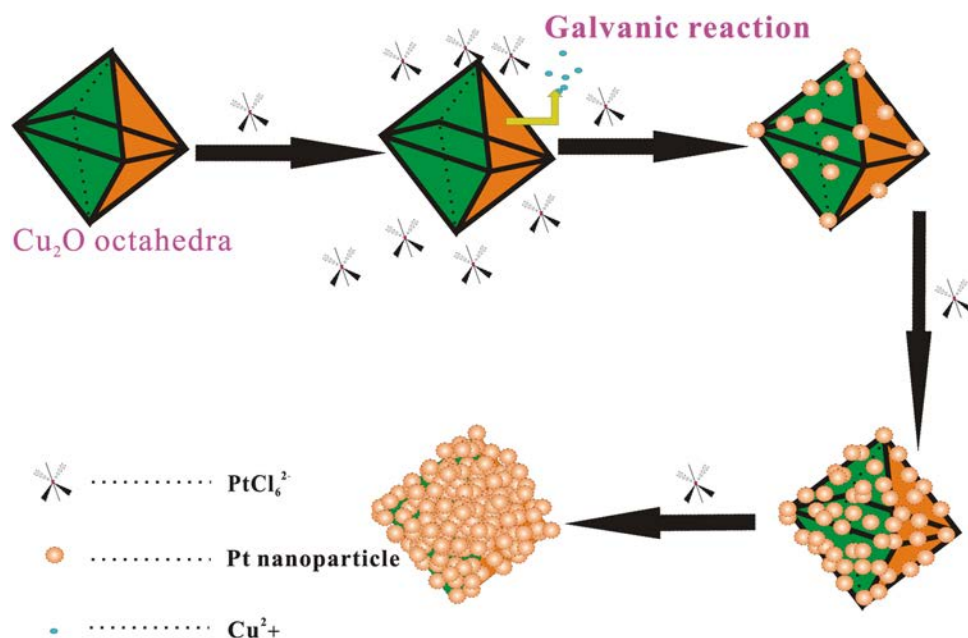
Up to now, the heterostructure with multilayer components is of significant interest and have been synthesized by several groups using Ag, Co, Te, Ni and Cu_2O nanostructures as templates usually via the galvanic replacement method.¹⁻³ In such constructions, each material retains its original properties, on the other hand, several new properties may be created due to its multiple heterostructure.

Therefore, these researches are of importance in discussing the components and have the opportunity to get multifunctional materials. A great quality of research efforts have been studied in the synthesis of these multistory structures and in studies of the optical properties. Meanwhile the plasma resonance properties of these nanostructures and the application in surface-enhanced raman scattering (SERS) were explored widely.⁴⁻⁶

In this study, we choose Cu_2O as sacrificial template. Cu_2O is a p-type semiconductor with a direct bandgap of 2.17 eV, and it has a maximum theoretical solar conversion efficiency of $\sim 12\%$ in a single layer photovoltaic cell.^{7,8} As a result of the special properties, Cu_2O has been considered as the promising material with potential applications in chemical reaction catalysis,⁹ photocatalysis,^{10,11} gas sensors,¹² solar energy conversion,¹³ templates,^{14–17} antibacterial activity,¹⁸ metal–insulator–metal resistive switching memory,¹⁹ cancer therapeutic agent. In the past decade, numerous scientific workers have paid great attention to the development of the noble metal– Cu_2O ,²⁰ meanwhile, to understand the mechanism of the progress within the reaction. Galvanic replacements have taken a vitally important role during the development of heterostructure nanocrystals. As we known, the redox pair value of $\text{PtCl}_6^{2-}/\text{Pt}$ (0.735 V) is much higher than $\text{Cu}_2\text{O}/\text{Cu}$ (-0.36 V), therefore, the Cu_2O crystals can be potentially used as the candidate for templates for the synthesis of multistory structure.²¹ But most important, it does not need any additive chemicals in this reaction progress. The formation process of heterostructure can be illustrated in Scheme 1.

Cu_2O was widely employed in photocatalysis, energy conversion, biosensor, etc. In our work, Cu_2O was introduced as the template for the growth of Pt to enhance the properties of the bi-layers

structure. As described above, the $\text{PtCl}_6^{2-}/\text{Pt}$ redox pair value is much higher than that of $\text{Cu}_2\text{O}/\text{Cu}$ and it is easy for PtNPs loading onto the facets of Cu_2O –Pt due to the galvanic reactions. Semiconductor materials (e.g., Cu_2O) can produce electron–hole pairs when exposed to light. In order to eliminate the electron–hole recombination phenomenon, PtNPs were controllably deposited onto the facets of Cu_2O to create Schottky barrier. Lots of holes were formed on semiconductor when electrons transferred from semiconductor to metal, which are linked with the difference of the Fermi energy. These electron–holes have capability of oxidizing and can be applied to photodegradation. Our study involve two primary mission: Growth of Cu_2O crystals with octahedron, and then the formation of $\text{Cu}_2\text{O}/\text{Pt}$ core/shell heterostructure in the H_2PtCl_6 aqueous solution. The method of the formation of Cu_2O crystals refer to previous researches.^{22–24} Hydrazine hydrate was employed to reduce Cu^{2+} to Cu^+ immediately in the water. Pt nanoparticles were obtained for the difference of the redox pair value between the $\text{PtCl}_6^{2-}/\text{Pt}$ and $\text{Cu}_2\text{O}/\text{Cu}$, and covered on the surface of Cu_2O , which is the key success of the formation of this novel structure. For the sake of structural stability of the template, we investigated the relationship between the amount of reductive agent and the morphology of Cu_2O , and then found optimum morphology for loading progress. Then, the galvanic reaction



Scheme 1. Schematic illustration of the growth of PtNPs on Cu_2O octahedron (color online).

between Cu_2O and Pt metal ions in H_2PtCl_6 solution was performed rapidly without any additive chemicals such as cetyltrimethyl ammonium bromide (CTAB). In our present work, Cu_2O -Pt hierarchical heterostructures with different amount of Pt precursor are obtained and their morphology, chemical and crystallographic properties were studied. In addition, in order to prove the improvement in photocatalysis of Cu_2O -Pt special structure, we make a contrast experiment for as-prepared Cu_2O and Cu_2O -Pt with varied concentration for the degradation of methylene blue (MB).²⁵ This phenomenon, maybe due to these heterostructures, can lead to photoinduced charge separation more efficiently.^{26,27} In our work, the purpose of this research is to develop a facile and green route to synthesize Cu_2O -Pt structure and study the role and mechanism toward the degradation of dye. The enhanced photocatalytic activity and the photo induced charge separation in these Cu_2O -Pt hierarchical heterostructures were demonstrated.

2. Experimental Method

2.1. Materials

Anhydrous copper (II) chloride (CuCl_2) and hydrazine hydrate ($\text{N}_2\text{H}_4 \cdot 2\text{H}_2\text{O}$) were obtained from Aladdin Chemistry Co., Ltd. Chloroauric acid ($\text{H}_2\text{PtCl}_6 \cdot 6\text{H}_2\text{O}$, 99.9%) was acquired from Shanghai Civi Chemical Technology Co., Ltd. MB was purchased from Tianjin Yongda Chemical Reagent Co., Ltd. Ethyl alcohol was manufactured by Hangzhou Gaojing Fine Chemical Co., Ltd. Deionized water was used for all solution preparations.

2.2. Synthesis of various morphologies of Cu_2O nanocrystals

The shapes of the Cu_2O nanocrystals that changed from octahedral to corrosive-octahedral structures were obtained through the reduction of CuCl_2 by $\text{N}_2\text{H}_4 \cdot 2\text{H}_2\text{O}$. About 3 mL of 0.5 M CuCl_2 solution was added to each beaker rapidly with the aid of vigorous stirring. A few minutes later, 3 mL of 5.0 M NaOH solution was added to the Cu^{2+} solution. Suddenly, the color of the solution turned to deep blue, indicating the formation of $\text{Cu}(\text{OH})_2$. Then, 15, 45, 85, 125, 210 and 320 μL of $\text{N}_2\text{H}_4 \cdot 2\text{H}_2\text{O}$ were quickly added into the blue solution. The solution changed to brownish yellow and these beakers were

kept stirring at room temperature for 10 min. The as-prepared Cu_2O nanocrystals were centrifuged at 7000 rpm for 6 min and deionized water was used to remove the unreacted chemicals by washing for 3 times. Finally, the chemical product was washed with 10 mL ethanol, and the precipitate was dispersed in 4 mL ethanol for the following characterizations.

2.3. Synthesis of Cu_2O -Pt hierarchical heterostructures with various Pt nanostructures

Cu_2O was used as template for the fabrication for the Cu_2O -Pt hierarchical heterostructures. Cu_2O octahedrons were dissolved in 50.0 mL deionized water, and then 0.0, 0.2, 0.5, 0.7 and 1.00 mL of 5.0 mM H_2PtCl_6 solution were, respectively dropwise added into the samples and labeled sequentially. Moreover, the beaker should be sealed to prevent O_2 penetrating into beaker. The solution changed from brownish yellow to black immediately, indicating the formation of Cu_2O -Pt heterostructures. The product solutions were placed on a magnetic stirrer at room temperature with vigorous stirring for 12 h. The Cu_2O -Pt heterostructures solution were centrifuged at 8000 rpm for 5 min and washed 3 times with deionized water to remove the impurity. Finally, the precipitate was dispersed in 4 mL ethanol for the following analysis.

3. Photocatalytic Activity Measurements

The photocatalytic degradation of MB aqueous solution was conducted at room temperature (25°C). The as-prepared Cu_2O -Pt hierarchical heterostructures were labeled a, b, c, d and e, meanwhile, 4 mg of the labeled Cu_2O -Pt hierarchical heterostructures were dispersed into 20 mL of MB aqueous solution (10^{-4}M), respectively. The mixture was magnetically stirred in the dark for 2 h to guarantee the absorption equilibrium of MB on the surface of the photocatalyst. About 4 mL solution was taken out for absorption measurements to obtain the initial data. As assist-catalyst, in the present experiment, H_2O_2 can easily be absorbed on the heterostructures surface and amplify the photoresponse to visible light. H_2O_2 was dropwise added into the solution as assist-catalyst. The H_2O_2 was dropwise added into the solution as assist-catalyst. A 20 W

lamp was used as the light source, while the distance was kept about 20 cm away from the solution. About 4 mL solution was taken out and centrifuged at 12 000 rpm to eliminate the photocatalyst for UV-Vis absorption measurements when the time interval was set. Finally, the 4 mL solution after the catalytic experiment was poured into the mother liquor.

4. Instrumentation

Field emission scanning electron microscopy (FE-SEM) images of the synthesized Cu_2O and Cu_2O -Pt hierarchical heterostructures were obtained using a JSM-6700F FE-SEM (JEOL, Japan). Transmission electron microscope (TEM) characterization was performed on a JEOL JEM-2100 electron microscope operating at 200 kV. X-ray diffractometer using a $\text{CuK}\alpha$ radiation source at 35 kV, with a scan rate of $0.02^\circ 2\theta \text{ s}^{-1}$ in the 2θ range of $20\text{--}90^\circ$. UV-Vis absorption spectra were acquired with the use of a Lambda 900 UV-Vis spectrophotometer (Perkin Elmer, USA). An X-ray photoelectron spectrometer (XPS) (Kratos Axis Ultra DLD) with an aluminum (mono) $\text{K}\alpha$ source (1486.6 eV).

5. Results and Discussion

The present growth progress of the novel structure is schematically illustrated in Scheme 1. Due to the

difference of the redox pair value between $\text{PtCl}_6^{2-}/\text{Pt}$ and $\text{Cu}_2\text{O}/\text{Cu}$, the PtCl_6^{2-} attached on the Cu_2O cuboctahedrons were reduced to Pt nanoparticles through Galvanic reaction. With more and more Pt nanoparticles deposited onto Cu_2O cuboctahedrons, finally this novel semiconductor-metal heterostructures were obtained. A series of morphologies of Cu_2O templates were obtained by changing the concentration of reductants in the progress of synthesizing the Cu_2O template. As shown in Fig. 1, clearly morphological evolutions of Cu_2O are obtained through changing the concentration of reductant. The Cu_2O cuboctahedrons were obtained at low amounts of reductive about $15 \mu\text{L}$, while $45 \mu\text{L}$ and $80 \mu\text{L}$ of reductants gave rise to Cu_2O octahedrons. As shown in Fig. 1, some wire-like products are observed at low concentration of reductants, and Cu_2O octahedrons with smooth facets and crystal edges are obtained when the amount of $\text{N}_2\text{H}_4 \cdot 2\text{H}_2\text{O}$ increased to $125 \mu\text{L}$. According to the literatures, these wire-like products are also Cu_2O crystals.^{28,29} With the further increase of the reductants, the facets of the Cu_2O octahedrons become irregular and rough with some holes and fissures.^{30–33} Bigger holes emerge and the facets of octahedral are damaged gradually when the amount increased to $320 \mu\text{L}$. In our previous reports, these phenomena are attributed to the excess amount of $\text{N}_2\text{H}_4 \cdot 2\text{H}_2\text{O}$ with the Cu_2O converting to Cu partially.³⁴

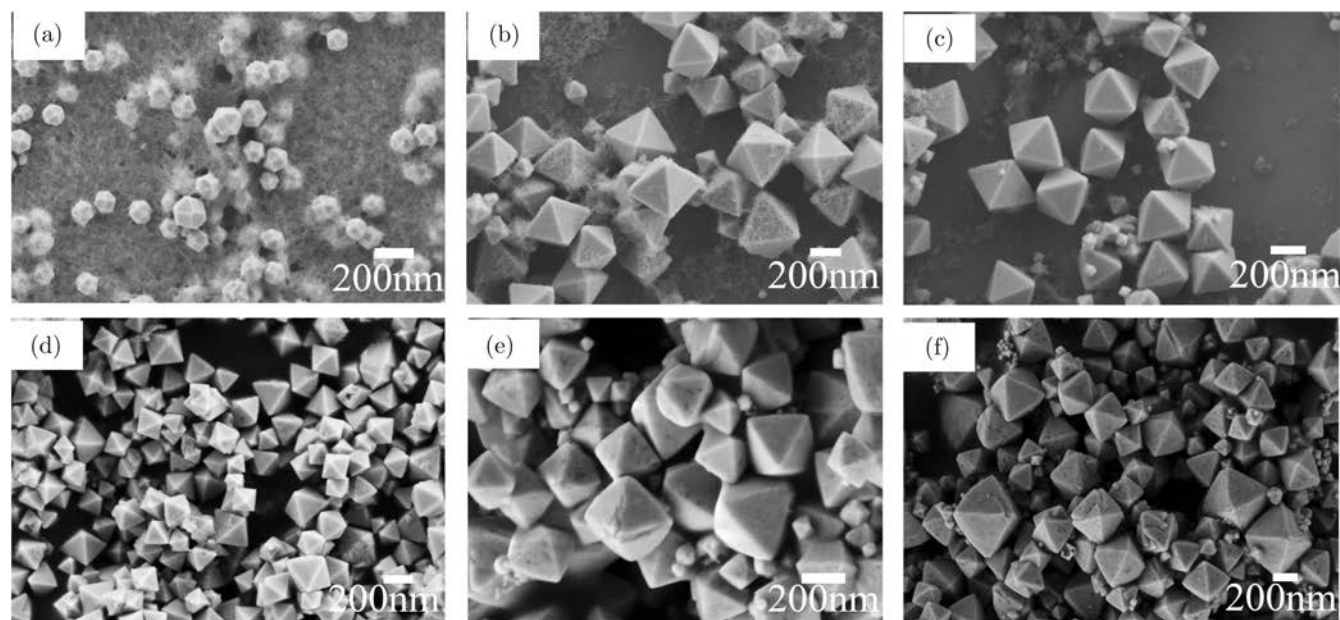


Fig. 1. FE-SEM images of the Cu_2O nanocrystals synthesized with morphological evolution by using different amounts of $\text{N}_2\text{H}_4 \cdot 2\text{H}_2\text{O}$. (a) $15 \mu\text{L}$, (b) $45 \mu\text{L}$, (c) $85 \mu\text{L}$, (d) $125 \mu\text{L}$, (e) $210 \mu\text{L}$, (f) $320 \mu\text{L}$.

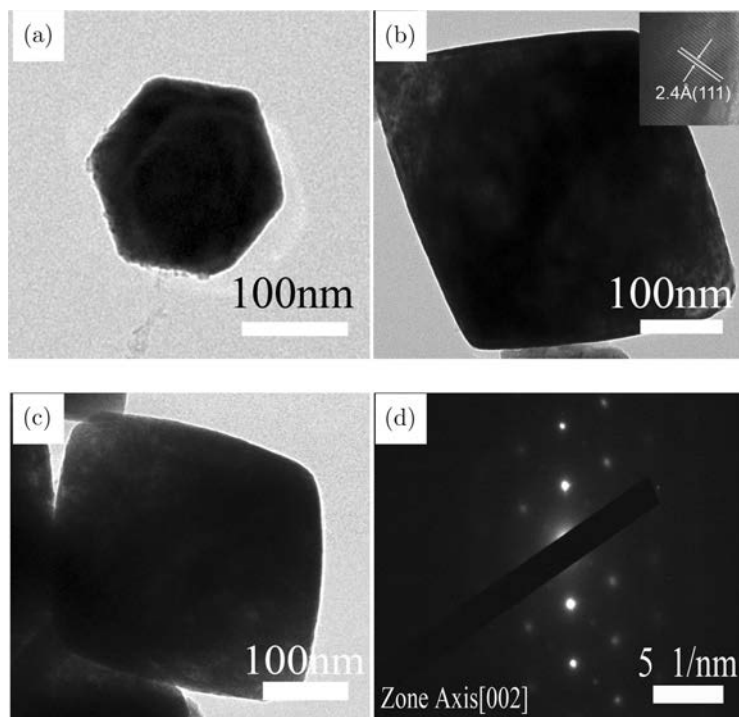


Fig. 2. TEM images of the square regions of (a) cuboctahedron, (b) octahedron and (c) corroded octahedron, (d) SAED patterns and HRTEM image of Cu_2O octahedron. The inset is the corresponding image of Cu_2O octahedron. The amounts of $\text{N}_2\text{H}_2 \cdot 2\text{H}_2\text{O}$ are 10 μL , 120 μL and 200 μL .

As exhibited in Fig. 2, octahedrons with smooth edges and corroded octahedrons bounded by eight $\{111\}$ facets, cuboctahedrons bounded by eight $\{111\}$ facets and six $\{110\}$ facets are obtained and the SAED patterns show the orientations of the corroded octahedrons [see Fig. 2(d)]. From Fig. 2(c), the surfaces and crystal edges of corroded octahedrons became rough and indistinct, which are according with Figs. 1(e) and 1(f). The HRTEM image shows that the lattice fringes with a spacing of 2.4 Å are ascribed to (111) lattice planes of Cu_2O , which are accordance with previous literatures.²⁴

The morphologies of the Cu_2O -Pt hierarchical heterostructures with various amounts of H_2PtCl_6 and the growth process were investigated by TEM and FE-SEM characterization. Figure 3 shows the Cu_2O -Pt hierarchical heterostructures with the morphological evolutions by increasing the amount of H_2PtCl_6 . From Figs. 3(a) to 3(d), with the amount of PtCl_6^{2-} increasing from 0.20 mL to 1.00 mL, galvanic reaction between Cu_2O and PtCl_6^{2-} become sufficient. With the continuous increasing amounts of H_2PtCl_6 , the Cu_2O octahedrons were encapsulated by PtNPs gradually and when the concentration arrived at 1.00 mL, the Cu_2O octahedrons

were completely surrounded by PtNPs tightly [see Figs. 3(e)–3(h)].

On the other hand, the PtNPs are very small with average diameter of 5 nm. The morphological evolution of these hierarchical heterostructures was presented from the TEM images [see Figs. 3(i)–3(l)]. Moreover, from these TEM images, a large amount of PtNPs ranging from 5 nm to 10 nm were densely grown on the Cu_2O facets to form shells about 30–50 nm.

To further confirm the presence of the PtNPs and analyze the crystal phase structures, the Cu_2O and Cu_2O -Pt power were characterized by XRD. XRD of the Cu_2O and Cu_2O -Pt were shown in Fig. 4. As shown in Fig. 4(a), all the diffraction peaks similarly located at 29.55, 36.42, 42.30, 61.34 and 73.53° can be considered as Cu_2O nanocrystals (JCPDS: 05-0677) and meanwhile, the peaks are according with the (110), (111), (200), (220), (311) crystal facets of Cu_2O . There is no other impurity peaks, indicating the pure phase of the Cu_2O nanocrystals.^{35,36} All the new emerging peaks, approximately locating at 40°, 46°, 67° and 81° and these new peaks were ascribed to Pt nanocrystals (JCPDS: 65-2868), which correspond to the (111), (200), (220) and (311) planes,

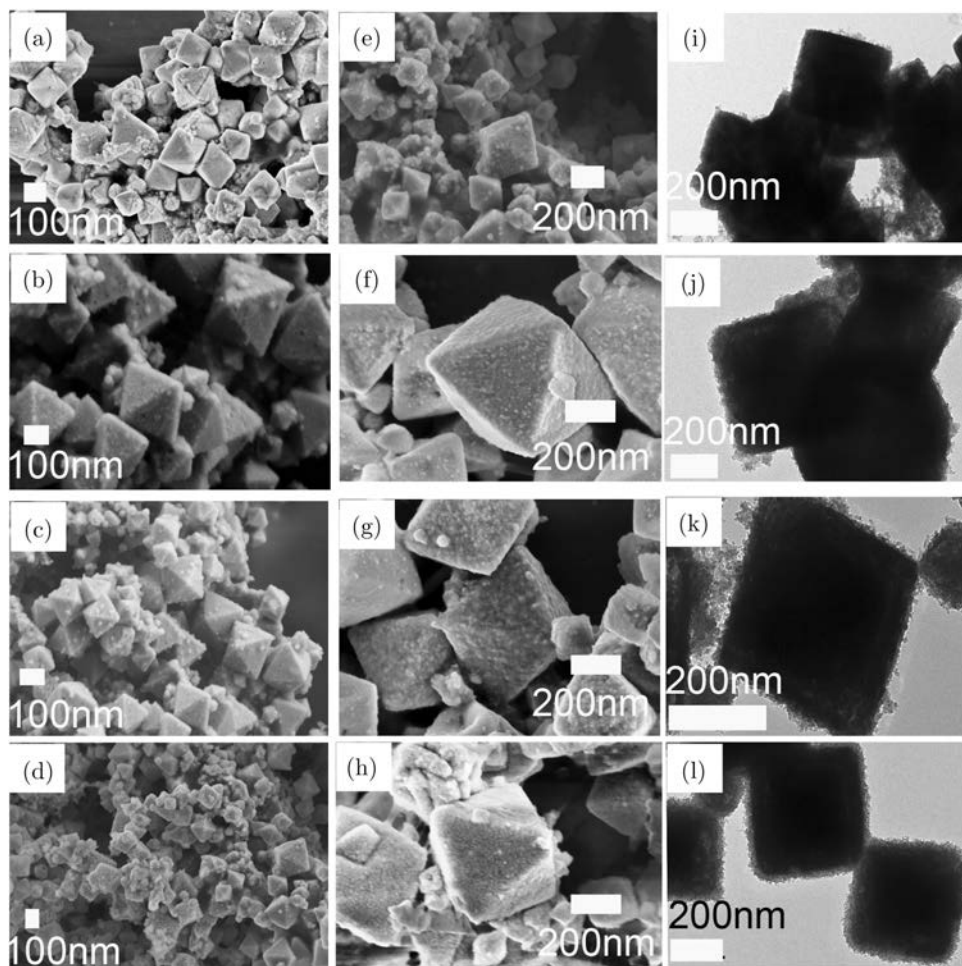


Fig. 3. FE-SEM images, TEM images of the surface growth of PtNPs on Cu_2O octahedron with increasing amounts of H_2PtCl_6 : (a), (e) and (i) 0.2 mL, (b), (f) and (j) 0.5 mL, (c), (g) and (k) 0.7 mL, (d), (h) and (l) 1 mL.

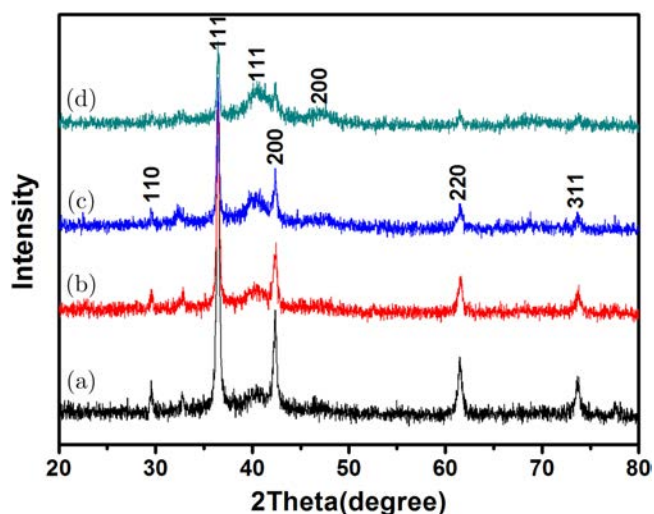


Fig. 4. XRD patterns of the Cu_2O -Pt heterostructures of the surface growth of PtNPs on Cu_2O octahedron with increasing amounts of H_2PtCl_6 : (a) 0.2 mL, (b) 0.5 mL, (c) 0.7 mL, (d) 1 mL (color online).

suggesting the successful formation of PtNPs.³⁷ It is conjectured that with the increasing volumes of H_2PtCl_6 , large numbers of PtNPs covered the surface of Cu_2O , resulting in the low-intensity signals of Cu_2O and the strong-intensity signal of Pt.²¹

XPS was further used to probe the surface chemical compositions and chemical oxidation state of the as-prepared Cu_2O octahedrons and Cu_2O -Pt hierarchical heterostructures (see Fig. 5). The core-level spectra of Cu 2p peaks were investigated by XPS [see Fig. 5(a)]. The Cu 2p peaks at binding energies of 932.1 eV and 952.1 eV were observed in the both the samples, which can be attributed to the binding energy of Cu 2p_{3/2} and Cu 2p_{1/2}, respectively.^{38–40} This confirms that the main composition of the hierarchical structure is Cu_2O . The peak at about 942.9 eV located at higher binding energy cannot be observed, which can be assigned to Cu^{2+} . The O 1s XPS spectra shown in Figs. 5(b) and 5(c)

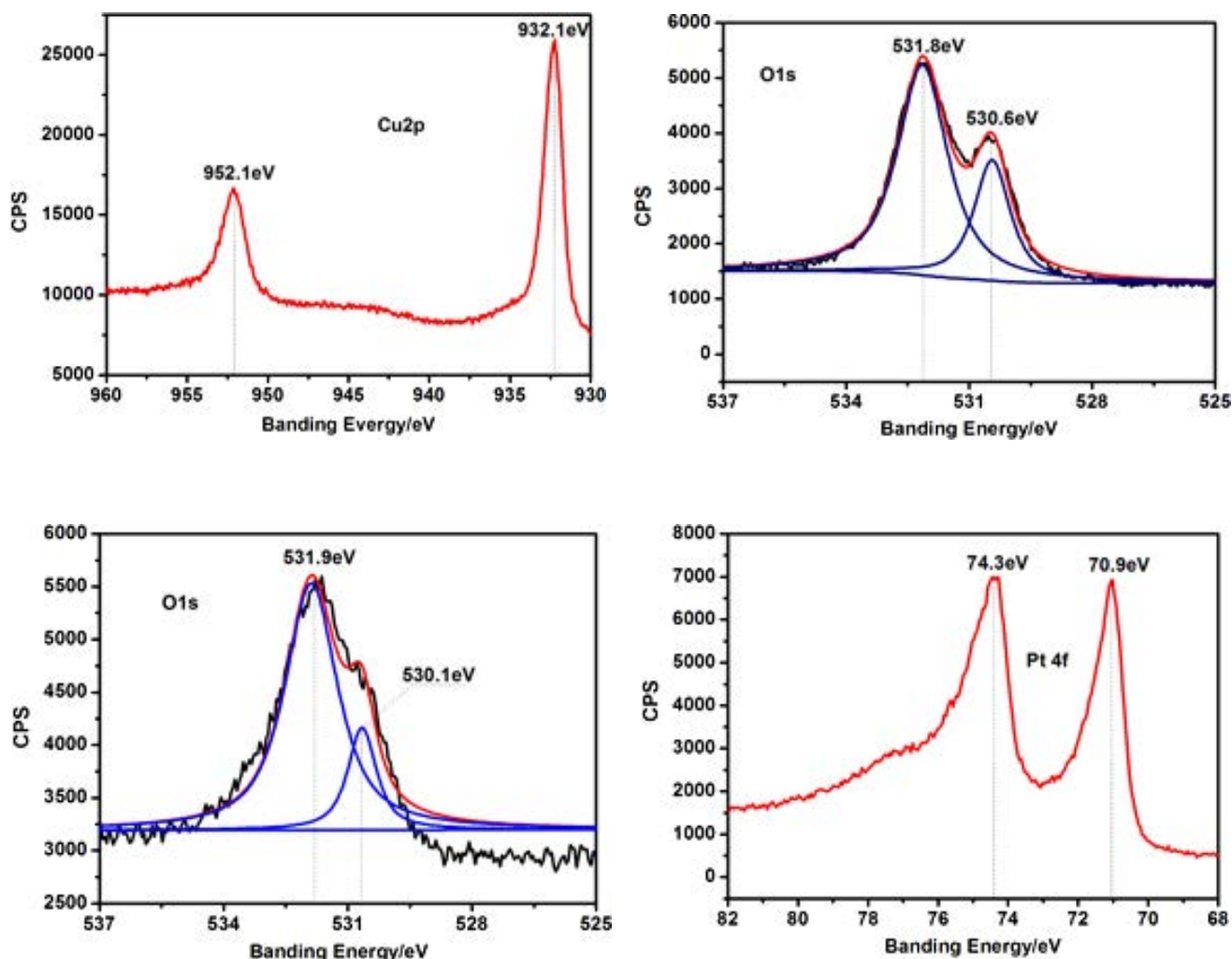


Fig. 5. (a) Cu 2p XPS spectra of Cu_2O octahedrons and O 1s XPS spectra of (b) Cu_2O octahedral, (c) Cu_2O -Pt hierarchical structures. (d) Pt 4f XPS spectrum of Cu_2O -Pt hierarchical structures (color online).

also provide more information about the galvanic reaction. As Fig. 5(c) shows, the broad peak of O 1s can be fitted by two peaks at binding energies of 531.8 eV and 530.6 eV. The peak at 530.6 eV is a characteristic of oxygen in metal oxide such as Cu_2O , CuO , and the 531.8 eV is assigned to other oxygen components such as OH, H_2O on the surface.³⁸ Comparing Fig. 5(b) with Fig. 5(c), it is obvious that the binding energy shift of O 1s from 530.6 eV to 530.1 eV in Cu_2O before and after galvanic reaction was attributed to the strong coordination between PtNGs and oxygen.⁴¹ Figure 5(d) shows the XPS spectrum in the Pt 4f region of the Cu_2O -Pt heterostructures. The two peaks at 74.3 eV and 70.9 eV are consistent with the binding energies of Pt 4f_{5/2} and Pt 4f_{7/2}, respectively.⁴² The

XPS results provide more details about the galvanic reaction and confirms that the Cu_2O -Pt hierarchical heterostructures have been prepared successfully.

A Schottky barrier can be created at the semiconductor-metal junction when controllably depositing metal nanoparticle onto semiconductors. When the electrons of Cu_2O were stimulated through light, the continuous transfer of electrons from semiconductor to metal nanoparticles will occur. Based on this theory, we believe that the novel semiconductor-metal heterostructures have excellent activity toward to the degradation of dye. In order to understand the role of Pt in enhancing the electron-holes separation and the photocatalytic of Cu_2O octahedrons and Cu_2O -Pt hierarchical structures were successfully prepared. A controlled comparative

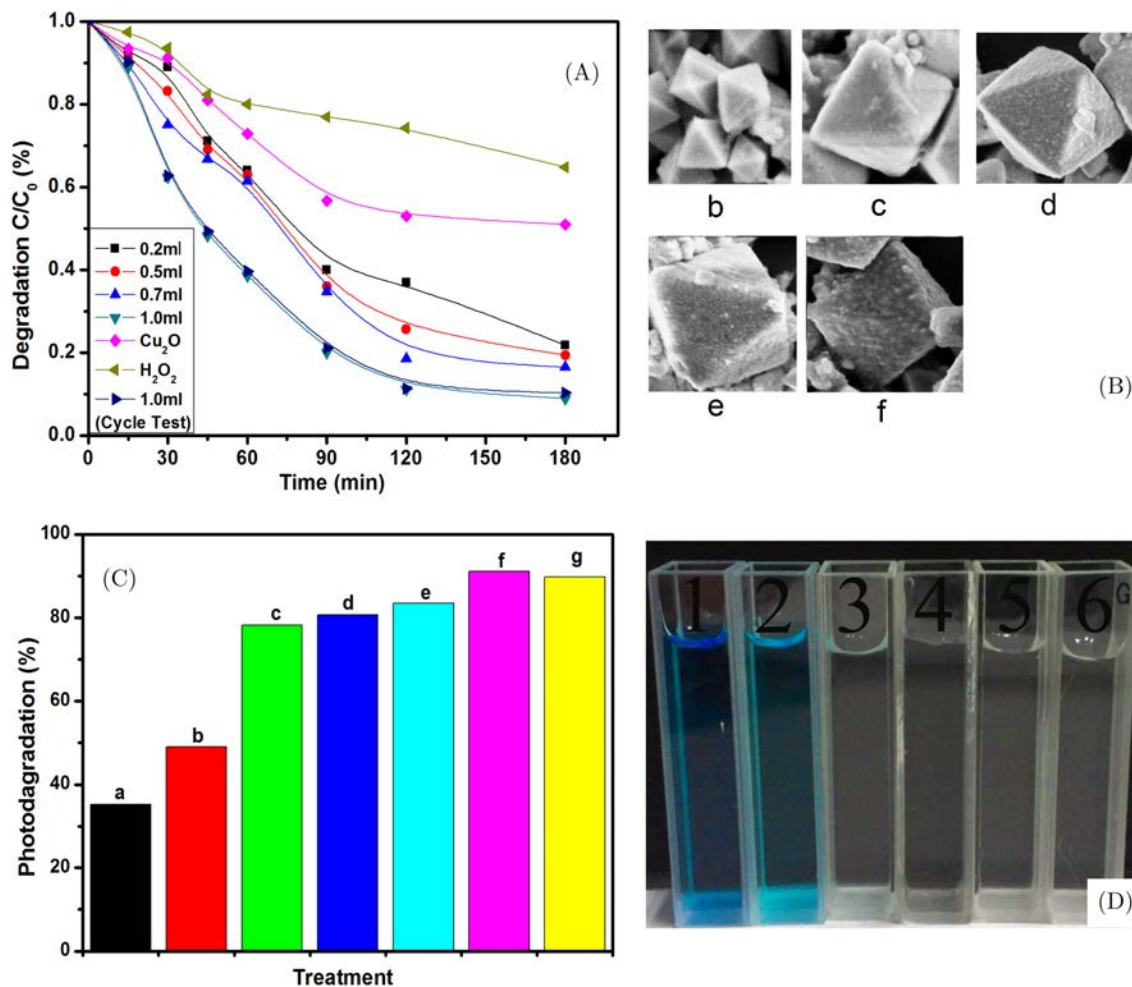


Fig. 6. (A) Degradation plots of MB with different photocatalysts: (a) H₂O₂ without any photocatalyst; (b) Cu₂O octahedral; (c) 0.20 mL, (d) 0.50 mL, (e) 0.70 mL, (f) 1.00 mL, (g) 1.00 mL H₂PtCl₆ (Cycle Test). (B) FE-SEM images of the corresponding photocatalysts. (C) Percentage photodegradation of MB of photocatalysts with different amounts. (D) Photographs of the MB solution after irradiation for 2 h (color online).

experiment toward the degradation MB was conducted to explore the improvement of Cu₂O–Pt hierarchical heterostructure in degradation.

Firstly, the Cu₂O octahedrons and Cu₂O–Pt hierarchical heterostructures were labeled with b, c, d, e and f, respectively. Then, the solutions including photocatalysts were utilized to degrade MB under visible light. Figure 6(a) shows the degradation plots of MB with different photocatalysts after visible light irradiation for 2 h. From Fig. 6(c), as expected, the photodegradation of MB was increased to 50% obviously with the presence of Cu₂O octahedrons, which is in accordance with the reports that Cu₂O have the ability to facilitate the degradation of MB. Meanwhile, due to the differences in the concentration of PtNPs, 78% to 96% of MB is photodegraded by Cu₂O–Pt with different concentration

of H₂PtCl₆, indicating that the photodegradation was mainly attributed to Cu₂O and Cu₂O–Pt. Therefore, the semiconductor–metal structure can improve the photodegradation activity due to the Schottky barrier and we can get the activity order of catalyst: Cu₂O–Pt (depend on concentration of H₂PtCl₆) > Cu₂O > H₂O₂. The color changes of the solutions are shown in Fig. 6(d).⁴³ Meanwhile, a cycle test was operated to test the recyclability of the novel catalyst. As the degradation C/C₀ and photodegradation shown in Figs. 6(A) and 6(D), the excellent recyclability of catalyst was demonstrated.

6. Conclusions

In summary, a facile approach was demonstrated to synthesize PtNPs immobilized on Cu₂O octahedrons

to form Cu₂O–Pt hierarchical heterostructures. FE-SEM, TEM, XPS and XRD were applied to study the morphology and the crystal structure of these products and explore the relationship between the amount of PtNPs and the morphology. In order to demonstrate the activity of semiconductor–metal structure in photodegradation, a comparative experiment was conducted. These Cu₂O–Pt hierarchical heterostructures showed enhanced photocatalytic activity due to the separation of electron/hole pairs.

Acknowledgments

We acknowledge the support of the project of National Natural Science Foundation of China (NSFC) (Grant number: 51243001) and Research Project of Department of Education of Zhejiang Province (Grant number: Y201122268).

References

- C. Liusman, H. Li, G. Lu, J. Wu, F. Boey, S. Z. Li and H. Zhang, *J. Phys. Chem. C* **116**, 10390 (2012).
- Q. P. Chen, J. H. Li, X. J. Li *et al.*, *Environ. Sci. Technol.* **46**, 11451 (2012).
- L. Wang, C. Clavero, Z. Huba *et al.*, *Nano Lett.* **11**, 1237 (2011).
- W. Xie, C. Herrmann, K. Kömpe, M. Haase and S. Schlücker, *J. Am. Chem. Soc.* **133**, 19302 (2011).
- C. Y. Song, J. Chen, J. L. Abell, Y. P. Cui and Y. P. Zhao, *Langmuir* **28**, 1488 (2012).
- M. R. Jones, K. D. Osberg, R. J. Macfarlane, M. R. Langille and C. A. Mirkin, *Chem. Rev.* **111**, 3736 (2011).
- L. N. Kong, W. Chen, D. K. Ma *et al.*, *J. Mater. Chem.* **22**, 719 (2012).
- Y. H. Liang, L. Shang, T. Bian *et al.*, *Cryst EngComm* **14**, 4431 (2012).
- B. X. Tang, F. Wang, J. H. Li, Y. X. Xie and M. B. Zhang, *J. Org. Chem.* **72**, 6294 (2007).
- Y. B. Wang, Y. N. Zhang, G. H. Zhao, H. Y. Tian, H. J. Shi and T. C. Zhou, *ACS Appl. Mater. Interfaces* **4**, 3965 (2012).
- J. Y. Zhang, H. L. Zhu, S. K. Zheng, F. Pan and T. M. Wang, *ACS Appl. Mater. Interfaces* **1**, 2111 (2009).
- J. T. Zhang, J. F. Liu, Q. P. X. Wang and Y. D. Li, *Chem. Mater.* **18**, 867 (2006).
- H. M. Wei, H. B. Gong, L. Chen, M. Zi and B. Q. Cao, *J. Phys. Chem. C* **116**, 10510 (2012).
- X. W. Liu, *Langmuir* **27**, 9100 (2011).
- W. C. Hou, L. Y. Chen and W. C. Tang, *Cryst. Growth Des.* **11**, 990 (2011).
- X. Wang and Y. D. Li, *J. Am. Chem. Soc.* **124**, 2880 (2002).
- L. Zhang, H. Jing, G. Boisvert *et al.*, *ACS Nano* **6**, 3514 (2012).
- H. T. Zhu, J. X. Wang and G. Y. Xu, *Cryst. Growth Des.* **9**, 633 (2009).
- S. D. Sun, X. P. Song, Y. X. Sun *et al.*, *Catal. Sci. Technol.* **2**, 925 (2012).
- L. Zhang, H. Jing, G. Boisvert, J. Z. He and H. Wang, *ACS Nano* **6**, 3514 (2012).
- F. Hong, S. D. Sun, H. J. You *et al.*, *Cryst. Growth Des.* **11**, 3694 (2012).
- S. Lee, C. W. Liang and L. W. Martin, *ACS Nano* **5**, 3736 (2011).
- Q. Hua, D. L. Shang, W. H. Zhang, K. Chen, S. J. Chang, Y. H. Ma, Z. Q. Jiang, J. L. Yang and W. X. Huang, *Langmuir* **27**, 665 (2011).
- H. Zhu, M. L. Du, D. L. Yu *et al.*, *J. Mater. Chem. A* **1**, 919 (2013).
- H. L. Zhu, J. Y. Zhang, X. Lan *et al.*, *Mater. Sci. Forum* **610-613**, 293 (2009).
- M. A. Mahmoud, W. Qian and M. A. El-Sayed, *Nano Lett.* **11**, 3285 (2011).
- W. W. Lu, S. Y. Gao and J. J. Wang, *J. Phys. Chem. C* **112**, 16792 (2008).
- W. W. Huang, L. M. Lyu, Y. C. Yang *et al.*, *J. Am. Chem. Soc.* **134**, 1261 (2012).
- Y. Xu, H. Wang, Y. F. Yu *et al.*, *J. Phys. Chem. C* **115**, 15288 (2011).
- H. L. Xu, W. Z. Wang and W. Zhu, *J. Phys. Chem. B* **110**, 13829 (2006).
- J. H. Kou and A. Saha, *Chem. Commun.* **48**, 5862 (2012).
- S. D. Sun, F. Y. Zhou and L. Q. Wang, *Cryst. Growth Des. Article* **10**, 541 (2010).
- F. Hong, S. D. Sun, H. J. You *et al.*, *Cryst. Growth Des.* **11**, 3694 (2011).
- Z. H. Ai, L. Z. Zhang, S. C. Lee *et al.*, *J. Phys. Chem. C* **113**, 20896 (2012).
- Q. Hua, D. L. Shang, W. H. Zhang *et al.*, *Langmuir*, **27**, 665 (2011).
- J. H. Zhong, G. R. Li, Z. L. Wang *et al.*, *Inorg. Chem.* **50**, 757 (2011).
- K. J. Tang, J. N. Zhang, W. F. Yan *et al.*, *J. Am. Chem. Soc.* **130**, 2676 (2008).
- A. Sarkar and A. Manthiram, *J. Phys. Chem. C* **114**, 4725 (2010).
- V. Subramanian, E. Wolf and P. V. Kamat, *J. Phys. Chem. B* **105**, 11439 (2001).
- B. Gates, Y. D. Yin and Y. N. Xia, *J. Am. Chem. Soc.* **122**, 12582 (2000).
- Y. Xu, H. Wang, Y. F. Yu *et al.*, *J. Phys. Chem. C* **115**, 15288 (2011).
- Y. Chang and T. J. H. Zeng, *Langmuir* **21**, 1074 (2005).
- B. Liu and H. Zeng, *J. Am. Chem. Soc.* **126**, 8124 (2004).